

Molecular extraction in single live cells by sneaking in and out magnetic nanomaterials

Zhen Yang^{a,b}, Liangzi Deng^a, Yucheng Lan^a, Xiaoliu Zhang^c, Zhonghong Gao^b, Ching-Wu Chu^{a,d,1}, Dong Cai^{a,1}, and Zhifeng Ren^{a,1}

^aDepartment of Physics and Texas Center for Superconductivity, University of Houston, Houston, TX 77204-5002; ^bSchool of Chemistry and Chemical Engineering, Huazhong University of Science and Technology, Wuhan, Hubei 430074, China; ^cCenter for Nuclear Receptors and Cell Signaling, University of Houston, Houston, TX 77204-5056; and ^dLawrence Berkeley National Laboratory, Berkeley, CA 94720

Contributed by Ching-Wu Chu, June 24, 2014 (sent for review May 15, 2014; reviewed by Donglu Shi and Lin Ji)

Extraction of intracellular molecules is crucial to the study of cellular signal pathways. Disruption of the cellular membrane remains the established method to release intracellular contents, which inevitably terminates the time course of biological processes. Also, conventional laboratory extractions mostly use bulky materials that ignore the heterogeneity of each cell. In this work, we developed magnetized carbon nanotubes that can be sneaked into and out of cell bodies under a magnetic force. Using a testing model with overexpression of GFP, the nanotubes successfully transported the intracellular GFP out at the single-cell level. The confined nanoscale invasiveness did not change cell viability or proliferation. This study presents the proof of concept of a previously unidentified real-time and single-cell approach to investigate cellular biology, signal messengers, and therapeutic effects with nanomaterials.

single-cell method | real-time detection | drug screening

Identification, quantification, and characterization of intracellular molecules in live cells are essential to the dissection of intracellular pathways and networks to understand physiology and pathogenesis at the cellular level (1–5). Cell lysis by disrupting the cellular membrane to release intracellular molecules is a conventional laboratory technique to prepare samples for analysis of genes, proteins, and metabolites (6–8). Due to the termination of cell lives, progressive information is lost. The inconsistency of molecular background in the cell preparations for samples at different time points largely compromises the study of cell differentiation, pathogenesis development, and therapeutic effectiveness. The extraction of intracellular molecules without killing cells so that repetitive sampling can be conducted at successive time points is becoming an imperative and urgent mission.

Additionally, cellular heterogeneity is frequently observed, particularly in cancer cells (9). However, the traditional biochemical analysis only provides the average of the cellular information with an ensemble of molecules from a large quantity of cells. Single-cell analysis is essential to obtain the physiological and pathological characteristics with respect to the genetic, proteomic, spatial, and temporal diversity of cells in cell biology and cancer research (10–12). Although microfluidics and laboratory-on-a-chip have been widely applied to single-cell manipulation via cell trapping, isolation, and sorting, analyte extraction still relies on complete lysis (13, 14).

Physical penetration of the cell membrane has exhibited low invasiveness in the extraction or release of intracellular molecules (15, 16). Nanoneedle and optoporation have been used for subcellular disruption and manipulation in living cells, but special and sophisticated setups are often required to wage the high spatial resolution and precise manipulation (17–20). Electroporation has also been demonstrated to release intracellular proteins without loss of cell viability (21). However, efficiency can be limited due to its dependence on diffusion to release the molecules. To date, the efficient extraction of molecules from live cells at the single-cell level remains a significant challenge in biotechnology.

Results and Discussion

Nanomaterials can be sneaked into and out of cells, and the fact that they can be transported across cell membranes during native biological processes or with negligible invasiveness is advantageous (22, 23). Previously we showed that highly efficient molecular delivery into cells was achieved by carbon nanotube spearing (24). Magnetized carbon nanotubes (MCNTs) driven by a magnetic force spear into cells and deliver molecular payloads. This method has demonstrated remarkable biocompatibility regarding cell viability, cell growth, cell cycle, DNA synthesis, cellular stimulation, and Akt and MAP kinase activities (25, 26). Given that the nanotube can enter cells without detectable perturbations, using it to extract molecules from live cells would be an appealing mode of exploration. Herein, we use MCNTs to transport intracellular molecules out of cells by magnetically driving them through the cells. The principle of intracellular extraction mediated by MCNTs through a cell is illustrated in Fig. 1A, where cells are cultured on a polycarbonate filter and later subjected to transfection of a GFP plasmid; Fig. 1B, where magnetic force is applied from the bottom of the cells, so that the MCNTs can first spear into the cells, and then travel through the cells and spear out; Fig. 1C, where, while traveling through the cellular cytoplasm, the MCNTs will have the chance to absorb GFP on their surfaces; and Fig. 1D, where a track-etched polycarbonate filter serves as a nanotube collector, and then the collected nanotubes with intracellular GFP

Significance

Current technical barriers in molecular sampling compromise the biomedical research regarding the diversity of cellular background. Usually hundreds and thousands of cells are lysed to release their contents. As such, the differences among individual cells are averaged out. The progressive cellular information can only be obtained by analysis of cells terminated at sequential time points, except by using external fluorescent and chemical labels that may interfere with pathways. We used biocompatible magnetic nanostructures to extract biomolecules from live cells. Nanomaterials were sneaked into and out of the cells, carrying with them molecules across the cell membrane without a significant impact on cell viability or proliferation. Our research suggests a previously unidentified avenue of intracellular interrogation to accurately capture the diversity of molecular information.

Author contributions: Z.Y. and D.C. designed research; Z.Y., Y.L., X.Z., and D.C. performed research; L.D. contributed new reagents/analytic tools; Z.Y., L.D., Y.L., Z.G., C.-W.C., D.C., and Z.R. analyzed data; and Z.Y., Z.G., C.-W.C., D.C., and Z.R. wrote the paper.

Reviewers: D.S., University of Cincinnati; and L.J., University of Texas, MD Anderson Cancer Center.

The authors declare no conflict of interest.

¹To whom correspondence may be addressed. Email: cwchu@uh.edu, dcai@uh.edu, or zren@uh.edu.

This article contains supporting information online at www.pnas.org/lookup/suppl/doi:10.1073/pnas.1411802111/-DCSupplemental.

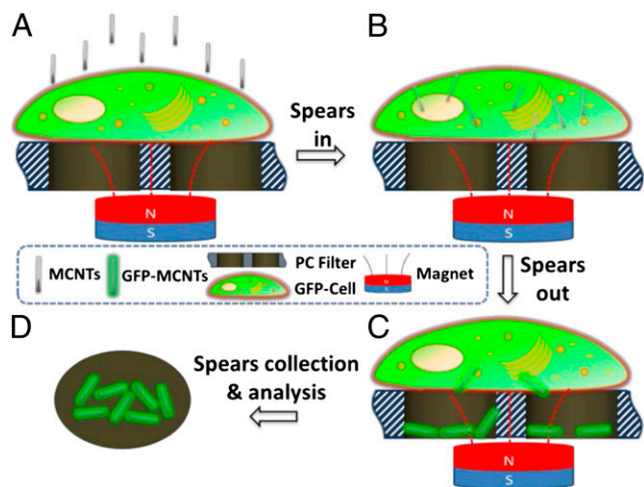


Fig. 1. Molecular extraction by spearing cells. (A) An external magnetic field drives MCNTs toward a cell cultured on a polycarbonate filter. To indicate the molecular extraction, the cell is transfected for GFP overexpression beforehand. (B) MCNTs spear into the cell under magnetic force. (C) MCNTs spear through and out of the cell and extract GFP. GFP-carrying spears are collected in the pores of a polycarbonate filter. (D) GFP representing the intracellular signal molecules can be used for analysis of individual pores.

are ultimately used for cellular analysis. This study pilots a previously unidentified approach for cellular signal interrogation with nanotechnology.

CNTs were grown with a plasma-enhanced chemical vapor deposition system, as previously described (27). The growth resulted in straight-aligned CNTs with magnetic Ni particles enclosed at the tips, making the CNTs magnetically drivable. To

make a cell-penetrating MCNT, the magnetization must be enhanced to generate higher magnetic force. Accordingly, a layer of Ni was deposited along the surface of individual CNTs by e-beam evaporation. However, Ni coating in biological applications exacerbates toxicity and hydrophobicity.

To reduce the toxicity of Ni-coated CNTs, the CNT array was connected to an electrochemistry system to conduct L-tyrosine electropolymerization on the surfaces of the CNTs (Fig. 2A). Studies by Marx et al. showed that electropolymerization of L-tyrosine is a feasible way to create a hydrophilic and biocompatible film that is suitable in diverse biological applications (28, 29). In the present study, we performed electropolymerization of L-tyrosine using cyclic voltammetry (CV) for 30 cycles (Fig. 2B). Analysis by the charge (Q) produced in each cycle reveals that Q decreases over time, indicating a self-limited growth of poly-L-tyrosine (Fig. 2C). This is similar to an electropolymerized, non-conducting polymer of phenol and its derivatives that are desirable to produce an ultrathin film on conducting electrodes (30, 31). The scanning electron microscope (SEM) image in Fig. 2D shows that Ni was preferentially deposited along the upper portions of the CNTs, which resulted from the vertical alignment of the CNTs and the intrinsically vertical deposition of e-beam evaporation. We also characterized the polymeric coating on the CNTs with transmission electron microscope (TEM) imaging. The images in Fig. 2E show a polymeric layer on the CNTs about 10 nm thick. The Ni layer is also observed in the TEM images.

To evaluate the magnetic properties, we measured the $M-H$ curve of the Ni-coated CNTs. It shows a saturated magnetization of ~ 4 electromagnetic units per gram ($\text{emu}\cdot\text{g}^{-1}$) (Fig. 2F). Minor magnetic hysteresis is also observed, which could be eliminated by replacing Ni with superparamagnetic materials. Meanwhile, the Ni-coated CNTs demonstrated a higher magnetic drivability in comparison with the as-made CNTs (Fig. S1). After the process, an aqueous suspension of the CNTs with Ni and poly-L-tyrosine modifications was prepared for the cell spearing experiment (Fig. 2G).

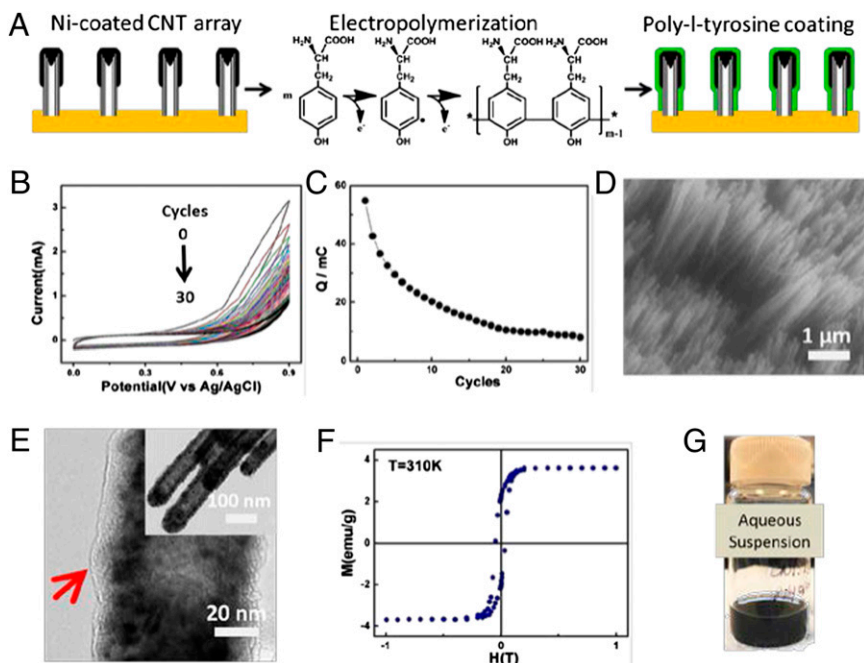


Fig. 2. Surface modification and characterization of MCNTs. (A) Schematic illustration of surface modification of MCNTs: Ni-coated CNT array by e-beam evaporation of Ni on the aligned CNT array, and poly-L-tyrosine coating by electropolymerization. (B) CV recording of the electropolymerization of L-tyrosine on CNTs with CNTs and Ag/AgCl as the working and reference electrodes, respectively. (C) Deposition charge (Q) (by integration of each cycle of CV) vs. the cycles. (D) SEM image of Ni-coated CNTs. (E) TEM images of Ni-coated CNTs whose surfaces have modified by poly-L-tyrosine coating (red arrow). (E, Inset) Low-magnification image. (F) Magnetization measurement of Ni-coated CNTs. (G) The aqueous suspension of magnetized MCNTs.

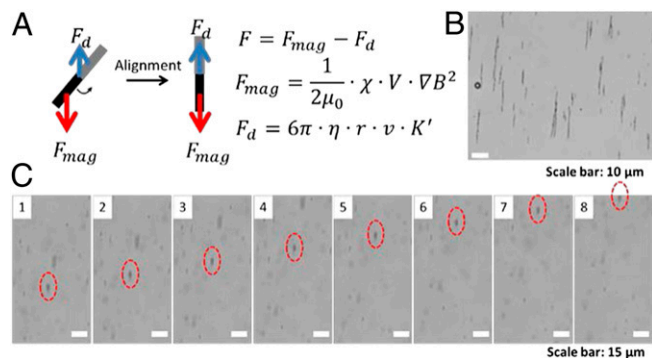


Fig. 3. MCNT response to magnetic force. (A) Force analysis of MCNTs in the magnetically guided spearing. The net pulling force (F) on the MCNTs is the summation of the magnetic force (F_{mag}) and the drag force (F_d) in liquid. In the equations that describe the forces, μ_0 is the magnetic permeability of free space, χ is the magnetic susceptibility of MCNTs, V is the volume of the nanotube, B is the magnetic field density, η is the viscosity of the liquid, r is the radius of the nanotube, v is the velocity of the MCNT in motion, and K' is the shape factor. (B) Microscopy image of MCNTs aligning in the magnetic field. (C) Movement of MCNTs by magnetic force. Images were taken over 8 s; numbers in the upper left corner (1–8) index the time. The same MCNT is circled in red in each of the eight images to show its movement.

As shown in Fig. 3A, the magnetically guided spearing by MCNT moves under the effect of two forces: magnetic force (F_{mag}) and drag force (F_d). The MCNTs are aligned with their polar axis in the direction of the magnetic gradient due to the unbalanced moments of F_{mag} and F_d . When aligned, the net pulling force (F) on MCNTs is F_{mag} minus F_d in liquid. Analysis of the force equations reveals that the thinner the MCNTs (i.e., smaller r) and larger the magnetic susceptibility (i.e., larger χ), the smaller the F_d and larger the F_{mag} , respectively, and ultimately, a larger net pulling F . With a microscope, we observed that MCNTs tandem attach in alignment to the magnetic field (Fig. 3B). Furthermore, we also evaluated the movement of MCNTs in the magnetic field under a microscope. The average speed was $\sim 12.7 \mu\text{m}\cdot\text{s}^{-1}$ according to their displacements in 8 s (Fig. 3C).

To evaluate the cell penetration by the MCNTs, cells of HEK293, a human embryonic kidney cancer cell line, were first cultured on a carbon-coated TEM sample grid pretreated with poly-L-lysine. After being speared for 10 min with a rare-earth magnet (0.355 T on the axis and 2 mm above the surface) following the procedure described in *Methods*, the cells were fixed and dehydrated for SEM inspection. The sample was viewed from both the top and bottom to reveal the nanotubes' entry into and exit from the cells, respectively (Fig. 4). However, SEM images are only capable of showing the MCNTs in the membrane, whereas MCNTs still inside or those that have escaped from the cells cannot be visualized. A recent study of interaction between 1D nanomaterial and cell membrane revealed a near-perpendicular entry mode and near-parallel adhesion mode (32). In our study, MCNTs were aligned to the magnetic pulling force. Thus, we speculate that the near-perpendicular entry mode is dominant at both entry into and exit from the cells. The near-parallel adhesion that appeared in the SEM images could be caused by the surface tension that results from the drying process in the preparation of SEM samples. Note that MCNTs in the bottom view had partially been speared out of the cell but were held by the carbon film of the TEM grid. With a culture substrate that has a larger opening, the MCNTs will exit the cell completely. In comparison with the top view, more fibrous structures were visible in the bottom view. They have dimensions similar to those of the original MCNTs, indicating an abundant host of MCNTs in each cell. According to the morphology of the speared cells (Fig. 4, *Middle*), the cells remain attached and

spread. This suggests retained integrity of the cell membrane and cytoskeleton that is usually lost in cells committing apoptosis or in necrosis.

To demonstrate the molecular extraction from single cells, a polycarbonate filter with 8- μm (diameter) pores was used as a culture substrate instead of a TEM grid. The pores trapped the exiting MCNTs from designated cells and kept them separated from cell to cell. A commercial lipofectamine kit was used to transfect the HEK293 cells at 90% efficiency for GFP over-expression in the cytoplasm. Thus, the extraction of intracellular GFP can be indicated by the appearance of GFP on the MCNTs. In Fig. 5A–C, the overlay of bright- and dark-field cell culture images showed cell alignment on and coverage of the pores. Most of the pores were covered by GFP-HEK293 cells. In Fig. 5D and E, pronounced green fluorescence can be observed in the MCNTs that speared into a pore. GFP is a soluble protein. It can attach to an MCNT in the form of a monolayer. Because the average size of a CNT is 1.5 μm in length and 100 nm in diameter, the maximum loading capacity of the GFP surface is 4×10^4 at a 4 nm in length by 3 nm in diameter. The result shows that MCNTs can carry intracellular molecules out of the cell while spearing through the cells. MCNTs in some neighboring pores exhibited no fluorescence, suggesting the absence of GFP-HEK293 cells over those pores. This evidence confirms the ability of the spearing method to differentiate molecular sampling at single-cell level. We also noticed that the MCNT collection in the pores was not consistent due to the variance of pore size (Fig. S2). Also, the number, type, size, and composition of target molecules affect extracting effectiveness by changing the interactions of MCNTs with the cytoplasm and cell membrane. However, these effects can be minimized by magnetically manipulating MCNTs.

Of major concern during the spearing-mediated molecular extraction is cell perturbation. A systematic study using flow cytometry to observe cell viability, cell growth, apoptosis, proliferation, cell cycle, and DNA synthesis has shown MCNTs' ability to be biocompatibly sneaked into a spectrum of cell types (25, 26). Because previous spearing did not include the process of cell penetration or the molecular extraction from the cells, we reevaluated some of the key issues, such as cell viability, apoptosis, and proliferation, in three groups of cells: speared

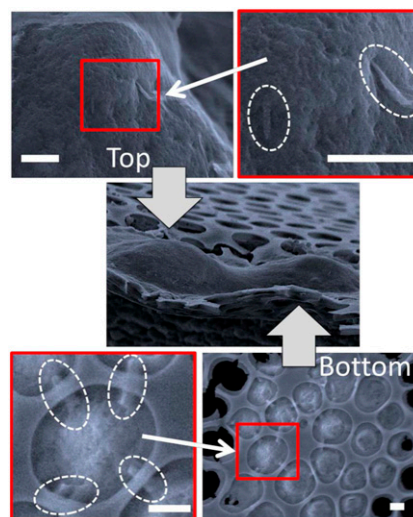


Fig. 4. MCNTs speared into and out of a cell viewed by SEM in top and bottom views. Local membrane surfaces appearing in the two red boxes are magnifications. Dashed circles highlight MCNTs positioned across the cell membrane. (Scale bars: 1 μm .)

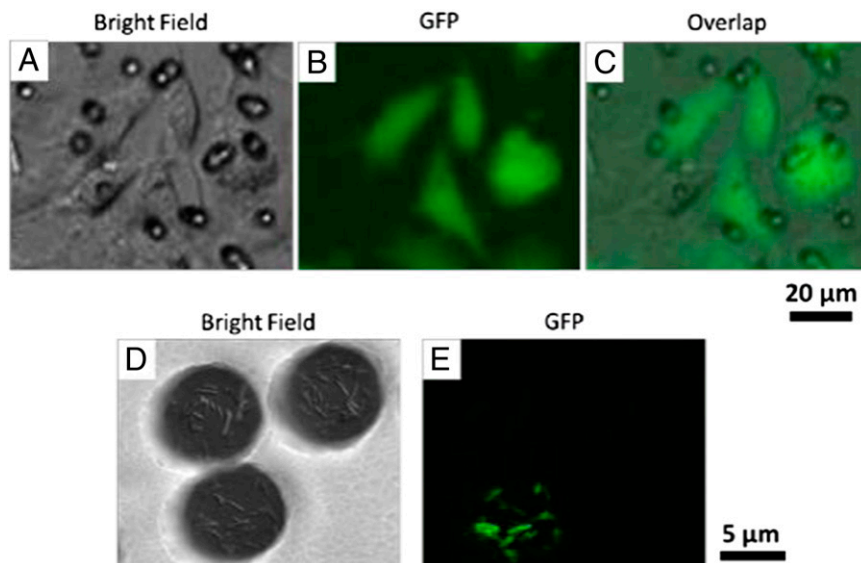


Fig. 5. Extraction of intracellular GFP via MCNTs spewed into cells. (A–C) Bright-field, dark-field, and overlapped images of GFP-transfected HEK293 cells on a polycarbonate filter, respectively. (D and E) Bright- and dark-field images of MCNTs spewed through cells and collected in the pores of a polycarbonate filter, respectively; the appearance of green fluorescence on MCNTs indicates that intracellular GFP was carried out of the cells by the MCNTs when spewed through cells.

(MCNT-spearing), magnetic field but no MCNTs (mag-only), and MCNT incubation but no magnetic field (MCNT-incubation). An Annexin V-FITC (KeyGEN Biotech) apoptosis detection kit and propidium iodide were used to dual stain cells for cytometry measurement. In Fig. 6, cell death and apoptosis were examined in the MCNT-spearing group and compared with the mag-only group, MCNT-incubation group, and a fourth group, the

12-h-after-spearing group. Propidium iodide enters a dying cell via leakage in a cell's plasma membrane. Spearing led to a slight drop in viability from 98.5% and from 98.2% to 96.4% for mag-only and MCNT-incubation, respectively. This suggests immediate recovery of the membrane after the spearing treatment in most of the cells. With cell culturing for 12 h, the propidium iodide positive rate returned, going from 3.3% to 1.4%, which is

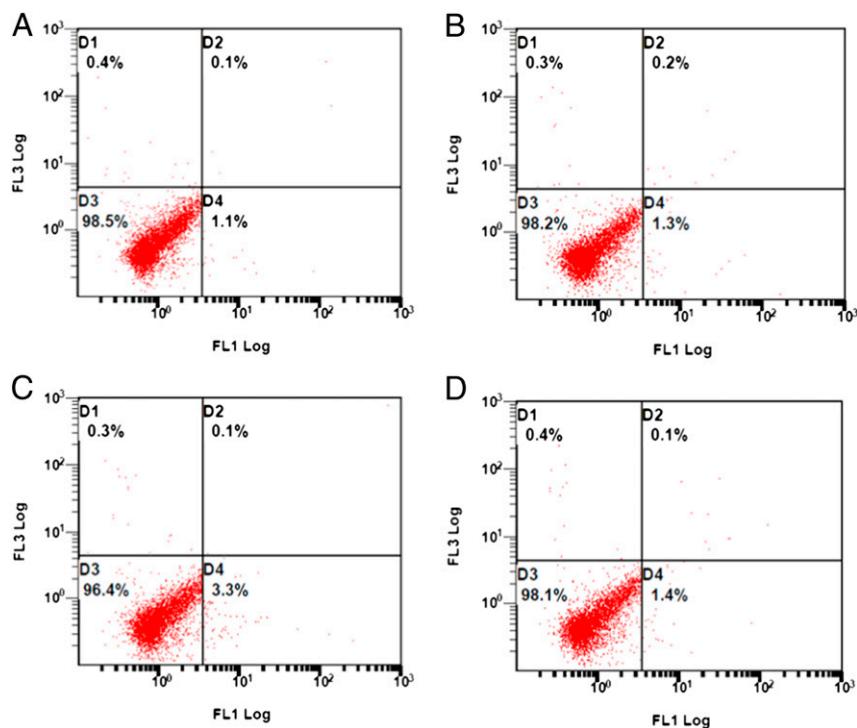


Fig. 6. Flow cytometry detection of cell viability and apoptosis in cells spewed by MCNT. (A) Mag-only group with normal culture under magnetic field. (B) MCNT-incubation group with MCNTs but without magnetic field driving. (C) MCNT-spearing group with MCNTs spewed out of cells by magnetic field driving. (D) Cells from the group in C but left in culture for 12 h after spearing. FL1, propidium iodide channel; FL3, Annexin V channel.

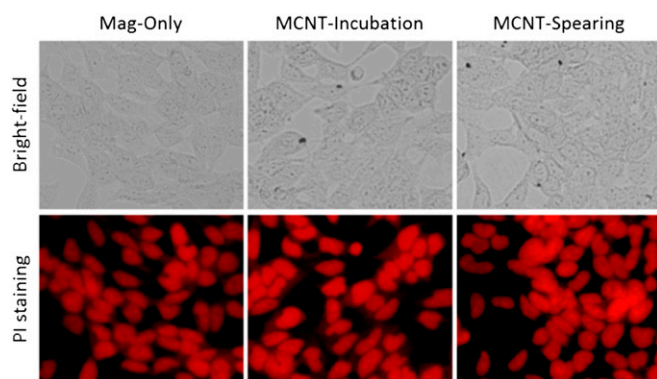


Fig. 7. Cellular morphology. (Upper) Bright-field images of the three groups of cells cultured for 24 h after spearing. The black chunks appearing in the MCNT-incubation and MCNT-spearing groups are the solid debris from the sample preparation. (Lower) The morphology of the nucleus in dark field. All cells were fixed before propidium iodide (PI) staining. Images are 300 μm in width.

close to the 1.1% level observed in the mag-only control. On the other hand, the Annexin V signal remained stable around 0.5% among all groups. This suggests that signal pathways related to programmed cell death are not interrupted by spearing. The three groups of cells were also compared 24 h after treatment. As shown, the morphology of cells in bright field (Fig. 7, Upper) exhibited no apparent differences. The nuclei were stained with propidium iodide after fixation (Fig. 7, Lower). Again, the size and shape of the nucleus did not show apparent differences. Cell density was estimated by nucleus count in randomly chosen fields. For the three groups of cells, the density was 53 ± 3 , 51 ± 6 , and 52 ± 2 per mm^2 ($n = 5$, mean \pm SD), respectively. This indicated the same proliferation rates among the groups. Taken together with the viability, cell death, and apoptosis results and the condition of the nucleus, the spearing method shows the biocompatibility needed to be applicable to sample intracellular molecules in live cells for the investigation of signal pathways.

In summary, we present the proof-of-concept of molecular sampling in single live cells with the successful extraction of intracellular GFP in transfected HEK293 cells. We show that MCNTs articulated with Ni coating and poly-L-tyrosine protection can be sneaked into and out of cells through the cell membrane without significant perturbations to cell viability and proliferation. By maintaining all cell conditions postspearing, repetitive molecular extraction to analyze cellular physiological and pathological signals in a longitudinal fashion will be possible. This research may provide a previously unidentified paradigm—nanomaterial-mediated molecular sampling in a live cell—thus potentially broadening the avenues for conducting single-cell study.

Methods

MCNT Preparation. A straightly aligned CNT array was obtained with an in-house, plasma-enhanced chemical vapor deposition system as previously described (25). Briefly, 10 nm Ni was deposited as the catalyst and produced CNTs of ~ 1.5 μm length with 10 min growth. The average diameter of the CNT was 100 nm. The CNT array was then placed in an e-beam evaporation system to deposit 20 nm Ni on the surface of the CNTs. The Ni-coated CNT array was connected to an electrochemical system equipped with three electrodes: MCNTs functioning as the working electrode, a Pt wire as the counter electrode, and Ag/AgCl as the reference electrode. An electrolyte solution was prepared by dissolving 3 mM L-tyrosine in a 0.1-M phosphate buffer (pH 6.5) containing 0.4 M NaCl. Electropolymerization of L-tyrosine was then conducted in CV with working electrode

potential ramping between 0 and 900 mV vs. the reference electrode. Thirty cycles of CV were run to thoroughly coat each MCNT with a poly-L-tyrosine layer. Finally, 1-h sonication was used to scraped MCNTs off the substrate, and a final aqueous CNT suspension was obtained with an estimated concentration of ~ 1 μM . To spear cells, MCNTs were centrifuged at 10,000 $\times g$ for 15 min and resuspended in a cell culture medium.

Cell Culture, GFP Plasmid Transfection, and Cells Speared by MCNTs. HEK293 cell lines were cultured in DMEM (Life Technologies) containing 10% (vol/vol) FCS and 100 U/mL penicillin–streptomycin in a humidified atmosphere ratio of 5% CO_2 and 95% air at 37 $^\circ\text{C}$. Cell culture substrates were sterilized with ethanol and surface treated by immersing in poly-L-lysine solution (1 mM in sterilized physiological phosphate buffer) overnight to facilitate cell adhesion. A polycarbonate filter (8- μm pore size; SterliTech) was first surface treated as described above and then used as cell culture substrates for SEM imaging and extraction experiments, respectively. For the extraction experiments, a commercial kit (Lipofectamine LTX with Plus Reagent; Life Technologies) was used to transfect the GFP plasmid into HEK293 cells cultured on the polycarbonate filter according to the manufacturer's protocol. Fluorescent images revealed that $\sim 90\%$ of transfected cells were GFP expressed. After GFP expression, 200 μL MCNT solution at a ~ 1 - μM concentration were added to the cell culture well, and a Nd-Fe-B permanent magnet was placed under the well at 0.355 T to spear MCNT through the cells. Magnetic force was applied for 10 min and then withdrawn by removing the magnet from the cell culture well.

Characterization. A JEOL 6330 SEM was used to conduct SEM imaging, including the morphology of Ni-coated CNTs and cells that were speared by MCNT. A JEOL 2010 SFX scanning TEM was used to observe CNT morphology with Ni coating and poly-L-tyrosine surface modification. For magnetization, the lyophilized powder of CNTs was obtained and measured with a Quantum Design Magnetometer equipped with a Superconducting Quantum Interference Device with an external magnetic field scanning capacity of -1 T to 1 T at 310 K. All optical images were obtained with an Olympus 1 \times 51 Inverted Fluorescence Microscope equipped with a 60 \times lens and a 40 \times oil objective lens. To observe the MCNT response to the magnetic field, a droplet of aqueous-suspended MCNTs was sealed between two glass slides for microscopy, and a Nd-Fe-B permanent magnet was placed adjacent to the glass slides to exert a planar pulling force on the MCNTs. A high-magnification image revealed the alignment of MCNTs in the magnetic field with the 60 \times oil objective lens and low-magnification images revealed the displacement of MCNTs in the magnetic field at different time intervals with the 40 \times oil objective lens. For SEM imaging, cells were fixed with a formaldehyde reaction (3.7% diluted with physiological phosphate buffer) for 10 min, and dehydrated by sequentially changing the concentration with 10%, 30%, 60%, 90%, and 100% ethanol solution (diluted with physiological phosphate buffer). Finally, cells on the TEM grid were dried and coated with 5 nm Au, and imaged using SEM (JEOL 6330F).

Cell Viability Evaluation. Three groups of cells were cultured to compare the effect of spearing on cell viability. Among these were the mag-only group with a normal cell culture and a Nd-Fe-B permanent magnet placed underneath, the MCNT-spearing group with 200 μL MCNTs of ~ 1 μM spearing cells that underwent 10 min pulling by a Nd-Fe-B magnet, and the MCNT-incubation group with 200 μL MCNTs of ~ 1 μM supplemented into the cell culture but no external magnet. For cytometry measurement, an additional group (a fourth group) was compared, i.e., the group containing cells that were incubated for an additional 12 h after the above spearing stimulus. Before flow cytometry, cells were collected with 0.25% trypsin. Collected cells were costained with 10 μM Annexin V-FITC and propidium iodide (Annexin V-FITC/PI kits). After 15-min dark:light incubation, cells were launched into cytometry (Beckman FC500) for cell death and apoptosis detection.

ACKNOWLEDGMENTS. Ms. Na Yin (School of Chemistry and Chemical Engineering, Huazhong University of Science and Technology) conducted flow cytometry measurements. The work in Houston is supported in part by US Air Force Office of Scientific Research Grant FA9550-09-1-0656, the T. L. Temple Foundation, the John J. and Rebecca Moores Endowment, and the State of Texas through the Texas Center for Superconductivity at the University of Houston.

1. Khakh BS, North RA (2006) P2X receptors as cell-surface ATP sensors in health and disease. *Nature* 442(7102):527–532.
2. Chen T, et al. (2013) DNA micelle flares for intracellular mRNA imaging and gene therapy. *Angew Chem Int Ed Engl* 52(7):2012–2016.

3. Khan J, et al. (2001) Classification and diagnostic prediction of cancers using gene expression profiling and artificial neural networks. *Nat Med* 7(6):673–679.
4. Jung T, Schauer U, Heusser C, Neumann C, Rieger C (1993) Detection of intracellular cytokines by flow cytometry. *J Immunol Methods* 159(1-2):197–207.

- Buchholz A, Hurlbaeus J, Wandrey C, Takors R (2002) Metabolomics: Quantification of intracellular metabolite dynamics. *Biomol Eng* 19(1):5–15.
- Zhang L, et al. (1992) Whole genome amplification from a single cell: Implications for genetic analysis. *Proc Natl Acad Sci USA* 89(13):5847–5851.
- Shi Q, et al. (2012) Single-cell proteomic chip for profiling intracellular signaling pathways in single tumor cells. *Proc Natl Acad Sci USA* 109(2):419–424.
- Rubakhin SS, Romanova EV, Nemes P, Sweedler JV (2011) Profiling metabolites and peptides in single cells. *Nat Methods* 8(Suppl 4):S20–S29.
- Spencer SL, Gaudet S, Albeck JG, Burke JM, Sorger PK (2009) Non-genetic origins of cell-to-cell variability in TRAIL-induced apoptosis. *Nature* 459(7245):428–432.
- Haun JB, Devaraj NK, Marinelli BS, Lee H, Weissleder R (2011) Probing intracellular biomarkers and mediators of cell activation using nanosensors and bioorthogonal chemistry. *ACS Nano* 5(4):3204–3213.
- Spiller DG, Wood CD, Rand DA, White MR (2010) Measurement of single-cell dynamics. *Nature* 465(7299):736–745.
- Wang D, Bodovitz S (2010) Single cell analysis: The new frontier in 'omics.' *Trends Biotechnol* 28(6):281–290.
- Joensson HN, Andersson Svahn H (2012) Droplet microfluidics—a tool for single-cell analysis. *Angew Chem Int Ed Engl* 51(49):12176–12192.
- Shah P, Zhu X, Chen C, Hu Y, Li CZ (2014) Lab-on-chip device for single cell trapping and analysis. *Biomed Microdevices* 16(1):35–41.
- Quinto-Su PA, et al. (2008) Examination of laser microbeam cell lysis in a PDMS microfluidic channel using time-resolved imaging. *Lab Chip* 8(3):408–414.
- Jeffries GD, et al. (2007) Using polarization-shaped optical vortex traps for single-cell nanosurgery. *Nano Lett* 7(2):415–420.
- Chen X, Kis A, Zettl A, Bertozzi CR (2007) A cell nanoinjector based on carbon nanotubes. *Proc Natl Acad Sci USA* 104(20):8218–8222.
- Kim W, Ng JK, Kunitake ME, Conklin BR, Yang P (2007) Interfacing silicon nanowires with mammalian cells. *J Am Chem Soc* 129(23):7228–7229.
- Yum K, Na S, Xiang Y, Wang N, Yu MF (2009) Mechanochemical delivery and dynamic tracking of fluorescent quantum dots in the cytoplasm and nucleus of living cells. *Nano Lett* 9(5):2193–2198.
- Li H, Sims CE, Wu HY, Allbritton NL (2001) Spatial control of cellular measurements with the laser micropipet. *Anal Chem* 73(19):4625–4631.
- Zhan Y, et al. (2012) Release of intracellular proteins by electroporation with preserved cell viability. *Anal Chem* 84(19):8102–8105.
- Kostarelos K, et al. (2007) Cellular uptake of functionalized carbon nanotubes is independent of functional group and cell type. *Nat Nanotechnol* 2(2):108–113.
- Deng ZJ, et al. (2013) Layer-by-layer nanoparticles for systemic codelivery of an anticancer drug and siRNA for potential triple-negative breast cancer treatment. *ACS Nano* 7(11):9571–9584.
- Cai D, et al. (2005) Highly efficient molecular delivery into mammalian cells using carbon nanotube spearing. *Nat Methods* 2(6):449–454.
- Cai D, et al. (2007) Carbon nanotube-mediated delivery of nucleic acids does not result in non-specific activation of B lymphocytes. *Nanotechnology* 18(36):365101.
- Cai D, et al. (2008) Interaction between carbon nanotubes and mammalian cells: Characterization by flow cytometry and application. *Nanotechnology* 19(34):1–10.
- Ren ZF, et al. (1998) Synthesis of large arrays of well-aligned carbon nanotubes on glass. *Science* 282(5391):1105–1107.
- Marx KA, Zhou T, Long D (2005) Electropolymerized films formed from the amphiphilic decyl esters of D- and L-tyrosine compared to L-tyrosine using the electrochemical quartz crystal microbalance. *Biomacromolecules* 6(3):1698–1706.
- Marx KA, Zhou T, McIntosh D, Brauhut SJ (2009) Electropolymerized tyrosine-based thin films: Selective cell binding via peptide recognition to novel electropolymerized biomimetic tyrosine RGDY films. *Anal Biochem* 384(1):86–95.
- Chen X, Matsumoto N, Hu Y, Wilson GS (2002) Electrochemically mediated electrodeposition/electropolymerization to yield a glucose microbiosensor with improved characteristics. *Anal Chem* 74(2):368–372.
- Yuqing M, Jianrong C, Xiaohua W (2004) Using electropolymerized non-conducting polymers to develop enzyme amperometric biosensors. *Trends Biotechnol* 22(5):227–231.
- Yi X, Shi X, Gao H (2014) A universal law for cell uptake of one-dimensional nanomaterials. *Nano Lett* 14(2):1049–1055.